J. Fluid Mech. (1967), *vol.* 27, *part* 3, *pp.* 595–608
Printed in Great Britain

The use of schlieren and shadowgraph techniques in the study of flow patterns in density stratified liquids

By D. E. MOWBRAY
Department of the Mechanics of Fluids, University of Manchester†

(Received 14 April 1966)

Various methods of establishing fluid media stably stratified in either temperature or the concentration of a foreign constituent are compared. A method used to construct a salt solution with precisely predetermined stratification is described. The Euler–Lagrange equations are solved exactly for a medium whose refractive index varies linearly in one dimension; the solution shows that a schlieren system may be used. For media with non-linear one-dimensional variation of refractive index, a modified shadowgraph technique may be employed. A device for the quantitative evaluation of a one-dimensional stratification is outlined and an example of its use is given.

1. Introduction

Characteristic diffusion times which govern the working life of an undisturbed stratified medium produced by (1) the mixing of a foreign gas in a gaseous medium, (2) the differential heating of layers of a gas or a liquid, and (3) the dissolving of a solute in a solvent, are compared. It is shown that the characteristic rate of diffusion of a solute in a solvent is several orders of magnitude smaller than the others. A technique for producing a salt-water medium with a given density stratification controlled to fine limits is described in §2.

The path of light rays through a medium whose refractive index varies only in one direction is analysed in §3 and an exact solution of the Euler–Lagrange equations is obtained. It is shown that for a linear variation of refractive index the path of a light ray is precisely a catenary, and that an incident parallel light beam passing through a glass walled tank containing such a medium emerges parallel so that a schlieren system may be used. This technique has been employed to observe wave motions reported in Mowbray & Rarity (1967).

For a non-linear variation of refractive index, a shadowgraph technique may be used; the shadowgraph image must be interpreted using the distorted image of a fine wire placed in the incident light beam. The distortion of the wire is measured directly and the data obtained used in a numerical solution of the Euler–Lagrange equations. The refractive index distribution is evaluated more easily and with greater accuracy than is possible with methods depending on light intensity measurements. An example of the technique is given for the determination of the refractive index distribution at the diffuse interface of two salt solution layers.

† Present address: Royal Aircraft Establishment, Bedford, England.

2. The production of density stratification

The principal requirements of a density-stratified fluid system for experimental flow investigations are that it should be reasonably easy to produce and that the stratification should be sufficiently long lived. For large systems the cost of production may be an important factor.

There are several ways of producing stratified fluids: by mixing gases of different densities, by differential heating of a layer of gas or liquid, or by varying the distribution of solute concentration in a solution. Thus a stably stratified stream can be produced continuously by steady release of carbon dioxide under air or by passing air through a grid of wires with differential electric heating placed in a wind tunnel. The coefficient of diffusivity, D, of carbon dioxide in air at 20 °C is 0·14 cm^2 sec^{-1} giving a typical length scale $(Dt)^{\frac{1}{2}}$ for diffusion of order 0·4 cm after 1 sec. The diffusivity of heat in air at 20 °C is 0·19 cm^2 sec^{-1}, giving a similar length scale. Density gradients produced in the laminar flow of air by either of these two methods will therefore decay rather quickly.

Webster (1964) used differential heating of the air stream in a wind tunnel to study the effect of stable density stratification on the decay of turbulence produced at a grid. In this case the turbulence itself will modify the vertical density profile which will consequently vary with distance from the grid. Ellison & Turner (1959, 1960) experimented on pipe and channel flows in which streams of brine were injected beneath a stream of water. A number of workers have studied multilayered flows in which layers of different density suffer little mixing and flows in water channels with differential heating. However, these techniques are not suitable for the production of deep layers with a uniform density gradient and will not be discussed further in the present paper which is concerned with the use of the last of the methods mentioned above.

This method owes its usefulness to the very low diffusivities of many solutes in solution; salts in water have diffusivities D of order 10^{-5} cm^2 sec^{-1} with corresponding length scales for diffusion $(Dt)^{\frac{1}{2}}$ of order 1 cm after 1 day. Density profiles in stratified solutions will therefore decay very slowly. It is difficult to produce such stratifications in a steady water channel flow, but they can readily be produced in a static tank.

The practical method of production of a specified density gradient in the tank depends upon the fact that the turbulence is strongly damped in a stable stratification. Thus thin layers of salt solution with successive increases in density can be run in one after another along the floor of the tank with relatively little mixing. Immediately after filling, the contents of the tank are layered with an approximate step-like distribution of density, but molecular diffusion of salt progressively diminishes these irregularities in the profile. This method which, with certain variations, has been used by a number of investigators can produce required density profiles with high accuracy.

The diffusion of a solute through a solvent satisfies Fick's law, which in one dimension is

$$(\partial/\partial t - D\,\partial^2/\partial y^2)C = 0$$

where C is the concentration, t the time and y the vertical space co-ordinate. The

coefficient of diffusion D is strictly a function of C, but for salt solution at room temperature this variation is small (figure 1) and the general features of the solution will be obtained assuming a constant value for D. The equation is then linear and of the same form as the one-dimensional heat conduction equation. Solutions of the equation must satisfy the condition that no salt crosses the boundaries. For the heat conduction equation this corresponds to the case of insulated boundaries. The solutions may be obtained using transform or Fourier series methods.

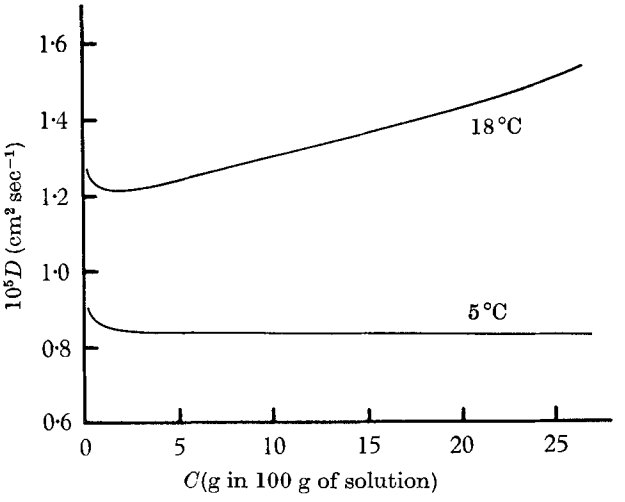

FIGURE 1. Diffusivity of aqueous salt solution as a function of the concentration of dissolved salt.

Of special interest is the linear density distribution, as this enables disturbances within the tank to be observed with a schlieren system. A linear density profile may be produced by filling the tank with a number of equal layers where the concentration is increased by equal amounts from the uppermost layer to the lowest layer. In the case of heat conduction this corresponds to many equal slabs of conducting material with equal steps in temperature from slab to slab and with insulated outer boundaries.

If the concentration of the rth layer from the top is originally $C_1(r-1)/(m-1)$, where m is the total number of layers, then at a later time the concentration is found to be

$$C = \tfrac{1}{2}C_1\left[1+\frac{4}{\pi(m-1)}\sum_{n=1}^{\infty} n^{-1}\exp\{-(n\pi/L)^2 Dt\}\cot(n\pi/2m)\cos(n\pi y/L)\right],$$

where y is the distance above the lower surface, L is the total depth and $n = 1, 3, 5, \ldots, \infty$.

Figures 2 and 3 show the development with time of the concentration profiles resulting from 10 and 20 layers. Only the upper half of the tank is shown as the profiles are symmetrical about the mid-level. The profiles are shown for five values of the dimensionless parameter $T = (\pi/L)^2 Dt$ where t is the time measured from the (hypothetical) instant of creation of the stepped density profile and L

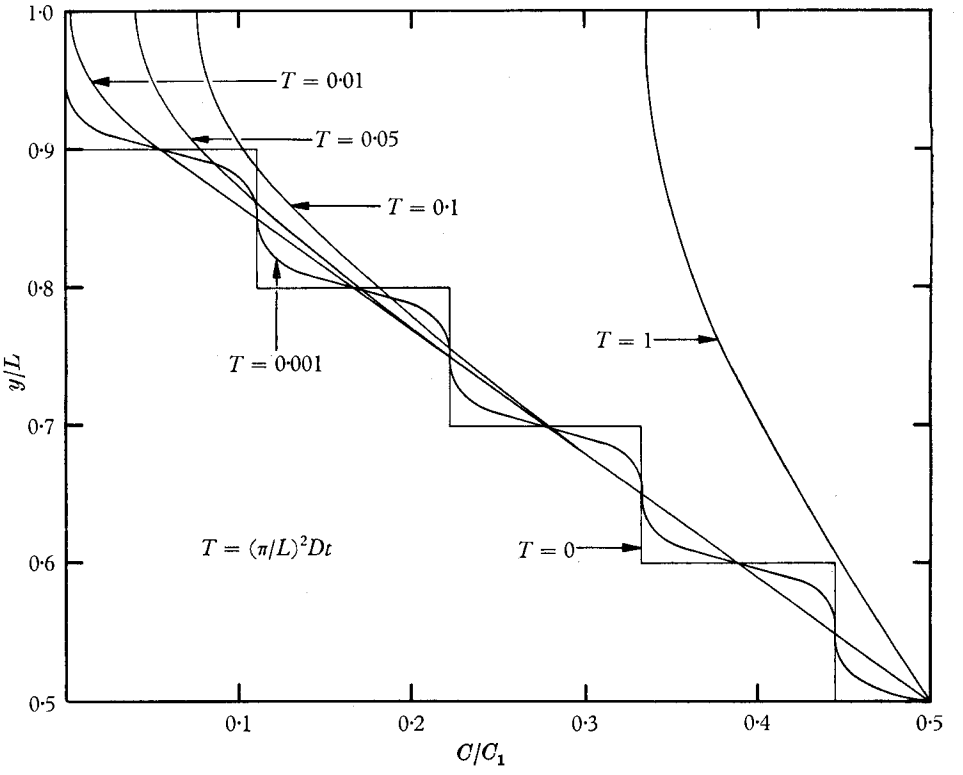

FIGURE 2. Development of the concentration profile from 10 layers.

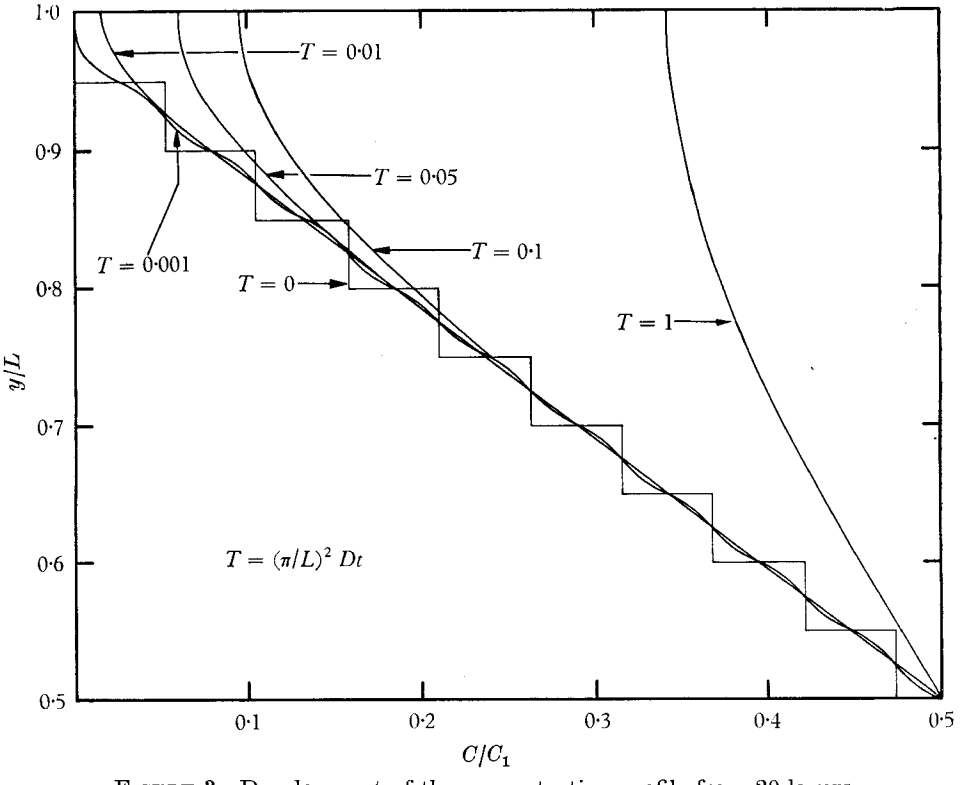

FIGURE 3. Development of the concentration profile from 20 layers.

is the depth of the tank. In both cases, all trace of the individual layers has disappeared by the time $T = 0{\cdot}01$ and the solution shows how a constant concentration gradient is produced in all of the tank except for regions close to the top (and bottom). As time increases, salt diffuses steadily through the region of constant gradient leaving the central region unchanged. However, the concentration of salt at the top is increased above the linear distribution and at the bottom the concentration is reduced as the concentration throughout the tank tends to a constant value.

Two diffusion times are involved in the process of maturing a stably stratified tank; the time for the individual layers to disappear and the time for the diffusion waves from the upper and lower boundaries to cross the tank. The time scale for individual layers is $L^2/(m^2\pi^2 D)$ and the time scale for the boundary effects to cross the tank is $L^2/(\pi^2 D)$. For the rapid production of a linear density distribution the number of layers should therefore be large, but the lifetime of the linear central region will depend entirely upon the depth of the tank. The density gradient is seen to be much more nearly linear for $T = 0{\cdot}001$ for the 20-layer system than for 10 layers although the growth of the diffusion wave is in both cases very similar. Calculations for a 30-layer system showed that all traces of the individual steps had disappeared for $T = 0{\cdot}001$. In terms of normal time for a stratified tank of salt solution 2 ft. deep, the values of $T = 0{\cdot}001$ and $0{\cdot}01$ correspond to times of 10·4 and 104 h respectively.

Observations indicate that linear profiles are established more rapidly than predicted theoretically. The differences are no doubt caused by small amounts of mixing of adjacent layers during the filling process. A small amount of mixing appears to smooth out the density discontinuities at each interface but leaves the central part of the layers unaffected. Since this configuration develops in the early stages of diffusion of a stepped system, further diffusion will produce the same linear distribution. The rate at which the salt solution is introduced into the tank is a compromise between too much interfacial mixing and an excessively long filling time. If the solution is introduced too quickly, a turbulent mixing region may extend upwards through several layers and it is impossible to identify the resulting distribution with one created from a system of discrete layers.

The linear profile may be extended towards the boundaries if half layers are used at the top and the bottom. If the linear part of the concentration profile is projected back, it is seen to cross the line $C/C_1 = 0$ at the value of y/L equal to the thickness of one-half layer. It should be noted that the linear concentration gradient dC/dy has a value of C_1/L when the half layers are used. When all the layers are of the same thickness, the value becomes $mC_1/(m-1)L$.

3. Flow observation and visualization

3.1. *Properties of solutions*

Of the many solutes and solvents that could be used, common salt and water have proved to be adequate for the present experiments. Valuable properties for experimental work are the near-linear relation of both the refractive index and the density with salt concentration. Furthermore, the solution remains clear

allowing the use of optical techniques and direct observation. There is a slight increase in viscosity: at 20 °C the viscosity of saturated salt solution is 1·700 centipoises compared with 1·005 centipoises for water. Although sugar provides a wider range of densities, it has the disadvantage that the viscosity increases rapidly with solute concentration. At 20 °C the density of a 60 % sugar solution is 1·286 g cm^{-3} and the viscosity is 56·5 centipoises. The cheapness of salt as a solute is partially offset by the precautions necessary to counteract the corrosive nature of salt and salt solution. The metallic parts of the experimental apparatus have to be of stainless steel or brass or alternatively coated with a corrosion resistant finish such as 'Araldite' epoxy resin.

Although many of the methods developed for the measurement of flow quantities in wind tunnels cannot be successfully adapted for use in stratified liquids, optical methods lend themselves extremely well. To measure velocities, bands of coloured dye or neutrally buoyant particles may be observed directly or photographically. Horizontal dye bands incorporated into the tank during the filling process are specially suited for the observation of internal waves. Alternate layers are coloured and although some of the colour does diffuse across the layer interfaces, the bands of colour remain distinct and their motions are easily observed.

Since changes in concentration are accompanied by small changes in refractive index, it is possible to use shadowgraph and schlieren methods usually associated with compressible gas flows. A disturbance in the stratified liquid will change the distribution of refractive index which in turn will cause a change in a shadowgraph or schlieren image. As the changes in refractive index are many times greater than those encountered in compressible gas flows, certain modifications must be made to the techniques.

The refractive index of salt solution is a function of temperature, the concentration of the dissolved salt and the wavelength of light. During experiments and beforehand, if diffusion has to take place, care is taken to avoid temperature changes of the solution in the tank. Two effects which have caused considerable disturbances are direct sunlight and the heat from the mercury vapour lamp used for the schlieren light source. In both cases, suitable shielding has proved to be an adequate remedy. In §3.3 on the schlieren system, the variation of refractive index with the wavelength of light is shown to have little or no effect on the final schlieren image. It is therefore sufficient to assume that the final shadowgraph or schlieren image is a result of variations of concentration only.

The refractive index, n, for light of wavelength 5893 Å in salt solution of density ρ g cm^{-3} at 18 °C is accurately represented by the linear relationship

$$n = 1{\cdot}3330 + 0{\cdot}231\,(\rho - 1),$$

or alternatively

$$n = 1{\cdot}1020 + 0{\cdot}231\sigma,$$

where $\sigma = \rho/\rho_{4\,^\circ C}$ is the specific gravity. The last expression for n should be compared with $n = 1 + 0{\cdot}000293\rho/\rho_{\text{N.T.P.}}$ given for sodium light in air by Beams (1955). These expressions for the refractive index of air and salt solution show that the changes of refractive index are of the order 1000 times larger for salt solution than for air. Thus, even in the case of very weak stratification, the

sensitivity of a schlieren system is normally more than adequate. Because of the large changes in refractive index, the differential equations governing the passage of light rays through the tank must be integrated exactly. Approximations made in the analysis of the optical records of compressible gas flows are no longer valid.

3.2. *Deflexion of the light by an undisturbed stratification*

The path of a light ray passing through a density inhomogeneity is determined by Fermat's law of stationary transit time. According to this law, the first variation of the integral along the ray path of the local refractive index $n(x, y, z)$ must vanish

$$\delta \int n(x, y, z)\, ds = 0, \tag{1}$$

where s is distance measured along the ray path. It can be shown (Beams 1955) that a ray path obeying (1) is described by the two differential equations for x and y as functions of z

$$x'' = \{1 + (x')^2 + (y')^2\}\left\{\frac{1}{n}\frac{\partial n}{\partial x} - \frac{x'}{n}\frac{\partial n}{\partial z}\right\}, \tag{2}$$

$$y'' = \{1 + (x')^2 + (y')^2\}\left\{\frac{1}{n}\frac{\partial n}{\partial y} - \frac{y'}{n}\frac{\partial n}{\partial z}\right\}, \tag{3}$$

where the prime denotes differentiation with respect to z.

These are known as the Euler–Lagrange equations and describe the ray path in regions where it does not encounter a discontinuity surface of $n(x, y, z)$. At such a surface the ray is deflected by a finite amount determined by Snell's law of refraction.

It is assumed that the liquid is bounded by vertical glass walls, free from distortion and inhomogeneities. The incident light is normal to the glass walls and this is chosen to be the z direction with $z = 0$ at the inside face of the first glass wall. Owing to the finite size of the light source the incident beam for both the shadowgraph and schlieren method consists of rays of light with slight inclinations to the z-axis; x'_e and y'_e. The subscript e refers to conditions at the inside face of the first glass wall. The y-axis is taken to be vertically upwards, the refractive index is then a decreasing function of y only, as variations of density (and therefore of refractive index) can only exist in the vertical direction when the fluid is undisturbed. Equations (2) and (3) therefore reduce to

$$x'' = 0 \tag{4}$$

and

$$y'' = \{1 + (x')^2 + (y')^2\}\frac{1}{n}\frac{dn}{dy}. \tag{5}$$

Upon integration (4) yields

$$x = x_e + x'_e z, \tag{6}$$

where $x' = \text{constant} = x'_e$. Relative to the x-axis the rays proceed without deviation from the point of entry x_e with their angle of entry.

Noting that

$$y'' = \frac{1}{2}\frac{d}{dy}(y')^2 = \frac{1}{2}\frac{d}{dy}\{1 + (x'_e)^2 + (y')^2\},$$

equation (5) is integrated to yield

$$1+(x_e')^2+(y')^2=(\alpha n/n_e)^2, \tag{7}$$

where $$\alpha=\{1+(x_e')^2+(y_e')^2\}^{\frac{1}{2}}.$$

If $\beta=\{1+(x_e')^2\}^{\frac{1}{2}}$ then integration of (7) yields

$$z=-\int_{y_e}^{y}\frac{dy}{\sqrt{\{(\alpha n/n_e)^2-\beta^2\}}}. \tag{8}$$

The negative square root is taken, since from (5) y'' is negative and thus y' is always decreasing and will in general be negative. If the distribution of refractive index is known, (8) may be evaluated in either closed form or numerically to give the trace of the ray path in the plane $x=x_e+x_e'z$.

3.3. *The schlieren system*

The schlieren system is a modified form of the twin concave mirror system normally used to observe disturbances in compressible gas flows. Light from a mercury vapour lamp passes through a condenser lens and is then reflected as a parallel beam by the first of the concave mirrors. After passing through the working section, the beam is brought to a focus by the second mirror. At this point, part of the light forming the image of the light source is cut off by a knife edge or graded filter while the remainder enters the schlieren camera which is focused on the working section of the tank. Any inhomogeneities in the working section cause the rays to be deflected either onto or away from the knife edge and the resulting changes in illumination of the camera image may be recorded. If it is intended to use the system to observe flows in stratified liquids, then the undisturbed density distribution in the working section must deflect all the rays by the same angle so that the beam incident upon the second mirror is composed of parallel rays. In practice, this requirement is fulfilled by a linear distribution of density. To intercept the beam, the second mirror is lowered and tilted and the knife edge and schlieren camera tilted to accept the beam. Disturbances within the working section cause perturbations of the light rays from this original configuration. The resultant changes in the intensity of illumination of the schlieren image correspond to regions of changed refractive index gradient and an interpretation of the image is obtained in the same way as for compressible gas flows.

If the working section contains a stable linear density distribution then the variation of refractive index may be expressed as

$$n=n_0-a(y-y_0), \tag{9}$$

where a is a positive constant and n_0 the known value of the refractive index at $y=y_0$.

With the change of variables $Z=a\alpha z/n_e$ and $N=n\alpha/\beta n_e$, equation (8) reduces to

$$Z=\int_{N_e}^{N}\{N^2-1\}^{-\frac{1}{2}}dN.$$

Hence $$Z=\cosh^{-1}N-\cosh^{-1}N_e$$

giving $$N=N_e\cosh Z+(N_e^2-1)^{\frac{1}{2}}\sinh Z, \tag{10}$$

where the root rejected does not satisfy (8). In terms of the original variables, (10) yields

$$y_e - y = (n_e/a)\{\cosh(a\alpha z/n_e) - 1 + \gamma \sinh(a\alpha z/n_e)\}, \tag{11}$$

where $\gamma = \{1 - (\beta/\alpha)^2\}^{\frac{1}{2}}$.

The inclination of the ray is

$$y' = -\alpha\{\sinh(a\alpha z/n_e) + \gamma \cosh(a\alpha z/n_e)\}. \tag{12}$$

Generally, (11) and (12) may be simplified without any measurable loss of accuracy. In the present experiments, the schlieren mirrors have a focal length of 180 in. and the light source is about $\frac{1}{4}$ in. across. This gives the maximum value of x_e' and y_e' as 1/720 of a radian. If the square of this quantity is neglected in comparison with unity then (11) and (12) yield

$$y_e - y = n_e\{\cosh(az/n_e) - 1\}/a$$

and

$$y' = -\sinh(az/n_e).$$

Furthermore, since az/n_e is generally less than 0·05, it is a good approximation to write

$$y_e - y = az^2/2n_e \tag{13}$$

and

$$y' = -az/n_e. \tag{14}$$

On leaving the liquid, the rays pass through the glass wall and into the air. At each interface the ray is deflected in accordance with Snell's law of refraction. For a ray which is at small angle to the normal, its deflexion is increased in the ratio n:1 where the refractive index of air is assumed to be unity and n is the refractive index of the fluid at the point where the ray leaves the tank. Since the value of $y_e - y$ as given by (13) is small, this value of n will be very close to n_e and from (14) the final deflexion of the rays will be

$$y' = -\alpha W, \tag{15}$$

where W is the width of the tank.

This simple result shows that the deflexion of the rays is independent of the point of entry. The beam is deflected downwards by an angle which is directly proportional to the gradient of refractive index. The error involved as a result of the approximations used to obtain (15) has a maximum value of 10^{-4} radian and in most instances is considerably less. Since 10^{-4} radian is considered to be the limit of sensitivity of this type of schlieren system, (15) may be regarded as being exact.

If the second mirror is placed at distance E beyond the second glass wall of the tank, then the displacement of the beam at the mirror will be WaE. Each time the tank is filled with a linear density distribution, the second mirror is placed below the level of the first by this amount. It is then possible to reflect the whole of the beam illuminating the undisturbed tank towards the knife edge and camera.

If the unfiltered light of a mercury vapour lamp is used for the light source, dispersion of the light rays causes the image of the light source at the knife edge to be distorted. The distortion is in the vertical direction only, since in the undisturbed tank this is the only direction in which the refractive index varies.

However, if all of the light forming this distorted image enters the camera, the image of the working section formed at the camera plate is of good quality. To produce the schlieren effect, part of the light forming the image of the light source must be cut off, either by a knife edge or a graded schlieren filter. Uniform darkening of the camera image is possible only if the knife edge is vertical. With a horizontal knife edge, the image becomes coloured, since the image of the light source is split into the colours of the spectrum and one colour is cut off more than any other. A horizontal knife edge may be used if the light is filtered, but this reduces the intensity of illumination considerably.

The schlieren method is restricted to the cases where the undisturbed density distribution is a linear function of depth. With other distributions, the emergent beam is not composed of parallel rays and a schlieren image cannot be formed. For cases where the stratification is a function of one space co-ordinate only, a modified shadowgraph method has been developed.

3.4. *Shadowgraph technique in stratified liquids*

A quantitative analysis of the usual shadowgraph record of a gas flow requires measurements to be made of light intensity. This is then followed by a numerical integration process to determine the distribution of refractive index that would give the measured distribution of intensities. A technique has been developed for stratified salt solution which eliminates the necessity for light intensity measurements and employs a simpler numerical process for the integration.

Direct measurements of the ray deflexions have been made in the determination of refractive index gradients by several investigators (Lamm, Svedberg & Peterson 1939). Usually these methods make assumptions which allow approximations to be made to the Euler–Lagrange equations. It should be noted that the result of (14) may be obtained directly from (3) if it is assumed that the refractive index and its gradient do not change along the ray path and also that the deflexion remains small. Equation (3) reduces to

$$y'' = -a/n$$

and so

$$y' = -az/n.$$

These approximations are usually valid only when the working section is quite narrow and the ray path in the liquid correspondingly short. In the present experiments the refractive index along a ray path may vary from 1·333 to 1·373, as the salt concentration increases from zero to saturated. Substituting these values into (7) the maximum possible deflexion is found to be 13·9°. In practice, deflexions in the region of 9° are frequently encountered in the region of a sharp increase in density.

A light source and concave mirror are used to illuminate the working section with a parallel beam as with the schlieren method. A fine steel wire is stretched across the first glass wall of the working section at 45° to the horizontal. Variations in refractive index within the working section produce a distorted image of the wire on an opaque screen placed at the second glass wall.

Since there are no horizontal variations of density each ray is deflected in a vertical plane and its displacement is easily determined as the vertical distance

between the distorted and the undistorted images of the wire. The measurements are made from a photographic negative of the screen. Some convenient length is marked on the screen to enable the magnification of the negative to be calculated. The displacements are then used as data in a digital computer programme which determines the distribution of refractive index.

3.5. *Integration of the Euler–Lagrange equations*

If x'_e and y'_e are zero then (7) gives

$$\int_{y_e}^{y_f} dy = -\int_0^W \{(n/n_e)^2 - 1\}^{\frac{1}{2}} dz. \tag{16}$$

The left-hand side of (16) is the displacement of the ray entering at $y = y_e$ and leaving the tank at $y = y_f$. The values of $y_f - y_e$ are the data obtained from the experiment and are known for all values of y_e.

An example of the method of solution for the determination of refractive index $n(y)$ is given for the case of a diffuse interface between two layers of salt solution of different density. The distorted image of the wire is shown in figure 4. Regions above and below the interface have constant values of refractive index. The graph shows that the rays are not deflected in these regions. For the purposes of computation, the origin of the y-axis is taken to be the level at which the refractive index of the lower layer is first affected by diffusion. The distance across the interface is divided into equal layers and the displacement of the rays measured at each layer. In this calculation the region is divided into 24 layers, this number being considered sufficient to accurately represent the main features of the distorted image curve.

Briefly, the distribution of refractive index in the lowest interval is determined and from this the refractive index in the next interval is predicted. Equation (16) is then integrated for the ray which enters at the top of the interval and which is deflected downwards into the predicted distribution. The integral is repeated with slight variations to the distribution until the correct displacement is obtained. This trial and error process is repeated for each interval until the interface has been crossed.

To start the computation, it is necessary to make some assumption about the initial variation of the refractive index. The variation is only small in the first interval and is probably closely represented by the quadratic form

$$n = n_0 - ky^2, \tag{17}$$

where n_0 is the constant value of the refractive index in the region below the interface and k is a small positive constant yet to be determined.

Equations (8) and (17) yield

$$W = \int_{y_{e1}}^{y_{f1}} \frac{dy}{\sqrt{[\{(n_0 - ky^2)/(n_0 - ky_{e1}^2)\}^2 - 1]}}, \tag{18}$$

where y_{e1} and y_{f1} are the points at which the ray enters and leaves the tank respectively.

If $ky^2 \ll n_0$, then (18) yields

$$k = n_0\{\tfrac{1}{2}\pi - \sin^{-1}(y_{f1}/y_{e1})\}^2/2W^2 \tag{19}$$

and

$$y_{f1} = y_{e1}\cos\{W\sqrt{(2k/n_0)}\}. \tag{20}$$

The second ray considered is that entering at $y_{e2}(y_{e2} = 2y_{e1})$. The variation in refractive index given by (17) is assumed to exist between $y = 0$ and $y = y_{e2}$, in

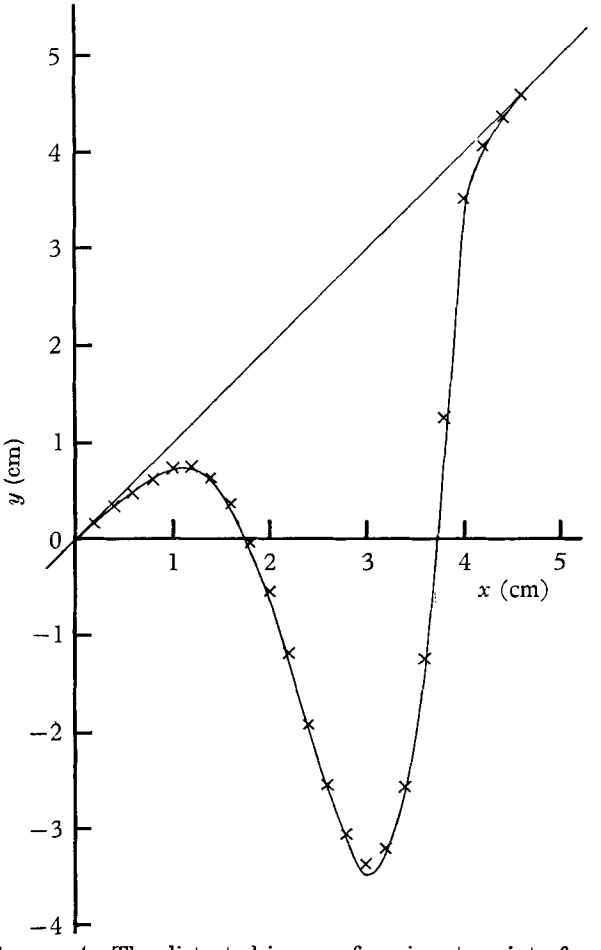

FIGURE 4. The distorted image of a wire at an interface.

which case (20) gives the point at which the ray emerges as $2y_{f1}$. If the displacement calculated in this way is not correct a change must be made to the value of the refractive index at the point where the ray enters. An increase in the displacement of the ray is achieved by increasing the gradient of refractive index and vice versa. It is therefore known whether the refractive index at y_{e2} is larger or smaller than the correct value, but the magnitude of the discrepancy has still to be determined. The value of n at y_{e2} is adjusted slightly and a quadratic is formed which has the new value of n at y_{e2}, the value given by (17) at y_{e1} and n_0 at $y = 0$. This quadratic for n is substituted into the integral of (16) and the value of the

integral is determined. (The difficulties associated with the evaluation of the integral are dealt with later.) This procedure is repeated until the displacement is sufficiently close to the measured value.

The value of the refractive index is now known at three points y_{e2}, y_{e1} and $y = 0$. The quadratic for n passing through these points is extrapolated to y_{e3} and the value of the integral determined. Should the result be incorrect, $n(3)$ is adjusted and a cubic fitted to the distribution at the four points. Using cubics in this way, the values of n are extrapolated and corrected at each layer until the region has been crossed.

An Adams–Bashforth fourth-order method is employed to determine the variation in y as equal steps in z are taken. However at $z = 0$, $y' = 0$ and after the first step has been taken, no change is obtained in the value of y and consequently in the value of n. The small changes that do occur over the first few steps must be determined using a higher derivative of y which is non-zero at $z = 0$.

Upon differentiation, (7) yields

$$y'' = (n/n_e^2)\,dn/dy.$$

At $z = 0$, $n = n_e$ and thus

$$y''_{z=0} = (1/n_e)\,(dn/dy)_{z=0}.$$

The value of $(dn/dy)_{z=0}$ is determined from four known values of n; at the point where the ray enters (this is a predicted value), and the three values of y immediately below y_e. It should be noted that

$$y''' = \frac{y'}{n_e^2}\left\{n\frac{d^2n}{dy^2} + \left(\frac{dn}{dy}\right)^2\right\},$$

which is zero at $z = 0$ since $y'_e = 0$.

The first few values of y are therefore predicted accurately by the Taylor series expansion

$$y = y_e + \tfrac{1}{2}(jh)^2 y''_{z=0},$$

where j is an integer and h the step length in the z-direction. Once these values of y are known the values of n and y' are calculated and the step by step integration may proceed. At each step the value of n is determined by Lagrangean interpolation of the known values of n at equally spaced intervals below y_e.

Figure 5 shows the distribution of refractive index obtained by the above technique from the curve of displacements shown in figure 4. For two equal layers of fresh water and salt solution of concentration C_1, the theoretical concentration profile is given by

$$C/C_1 = \frac{1}{2}\left[1 - \frac{4}{\pi}\sum_{n=1}^{\infty}\frac{1}{n}(-1)^{\frac{1}{2}(n+1)}\exp\{-(n\pi/L)^2 Dt\}\cos(n\pi y/L)\right] \quad (n = 1, 3, 5, \ldots).$$

However this profile will be slightly modified as a result of the mixing at the interface during the filling process. In view of this it is impossible to check the computed result theoretically, but a test has been carried out by taking the refractive index profile of figure 5 and calculating the corresponding ray deviations. Points from this solution are marked with crosses in figure 4 and it is seen that the agreement is satisfactory.

A reduction in the amount of computation is possible if (7) is written as

$$z = -\int_{y_e}^{y_f} \frac{dy}{\sqrt{\{(n/n_e)^2 - 1\}}}$$

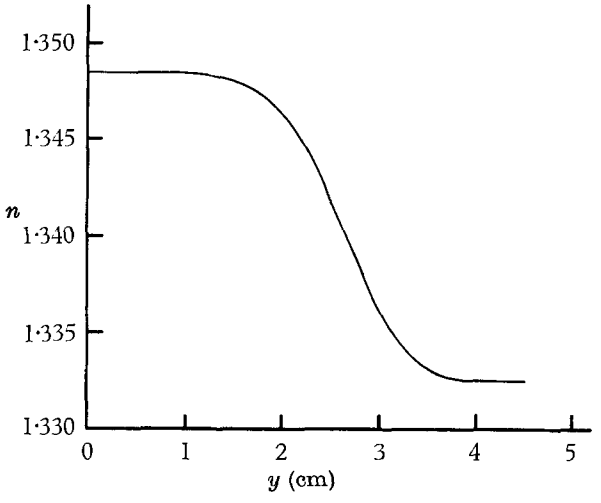

FIGURE 5. The computed distribution of refractive index.

and integrated in equal steps of y using a Gauss integration formula. This is possible as the value of the refractive index is known at equally spaced values of y less than y_e and interpolation for the refractive index and the calculation of dy/dz and dn/dy is no longer necessary. A value of n_e is predicted and the integration performed to determine z. The value of n_e is adjusted until the value of z becomes close enough to W, the width of the tank. The integrand becomes infinite at $y = y_e$ but this difficulty is overcome by using an integration formula for functions behaving like $x^{-\frac{1}{2}}$ as $x \to 0$. Although this method is a saving in the case of a one-dimensional profile, work is progressing with the extension of the technique to two dimensions where it appears that the integration will have to be carried out using the method described in the above section.

The author would like to express his thanks to Professor N. H. Johannesen for the help given and the interest shown in the work. He has also had many helpful discussions with Dr B. S. H. Rarity and Dr B. R. Morton. During the period of the work the author was in receipt of a Science Research Council maintenance grant. Acknowledgement is also made to the Ministry of Aviation who supported this work.

REFERENCES

BEAMS, J. W. 1955 *Shadow and Schlieren Methods.* High Speed Aerodynamics and Jet Propulsion. **9**, 22–44. Oxford University Press.

ELLISON, T. H. & TURNER, J. S. 1959 *J. Fluid Mech.* **8**, 514.

ELLISON, T. H. & TURNER, J. S. 1960 *J. Fluid Mech.* **8**, 529.

LAMM, O., SVEDBERG, T. & PETERSON, P. O. 1939 *The Ultracentrifuge.* Oxford University Press.

MOWBRAY, D. E. & RARITY, B. S. H. 1967 (To be published.)

WEBSTER, C. A. G. 1964 *J. Fluid Mech.* **19**, 221.